

Residual Strength Improvement of an Aluminium Alloy Cracked Panel

F. Caputo*, G. Lamanna and A. Soprano

Department of Industrial and Information Engineering, Second University of Naples, via Roma 29 - 81031 Aversa, Italy

Abstract: This work deals with the application of the micromechanical Gurson-Tvergaard (GT) model to the determination of the residual strength of an aluminium flat stiffened panel (2024 T3) with a central through crack, by means of finite element simulations. The load condition is represented by a monotonic traction along the direction orthogonal to the crack plane. The used Finite Element code is WARP 3D[®], which allows simulating ductile damage propagation by considering the GT model.

Numerical results have been compared with experimental ones available in literature. In the second part of the work, a home made procedure founded on the SDI (Stochastic Design Improvement) technique is presented and applied to the improvement of the residual strength properties of the considered panel.

Keywords: Fracture mechanics, Gurson model, R-Curve, SDI.

INTRODUCTION

The availability of prediction numerical tools for the determination of the R-curve of cracked structure improves the capabilities of the designers to deeply investigate on the residual strength properties of such structures.

Within this work, a micromechanical approach has been followed, by considering a numerical model that is able to explain the characteristic material behaviour from the crack onset up to the final failure of the considered component, without suffering any dependence on the current geometry.

Ductile fracture arises in many ferrous and non-ferrous alloys through the nucleation of cavities produced by the fragile breaking or decohesion of inclusions [1, 2]. When such cavities begin to grow in size, they cause local severe stress-strain fields in the surroundings of small inclusions, thereby nucleating small-scale cavities which participate to the final phase of the coalescence process and therefore to the macroscopic crack growth. The process of cavity growth is well understood and the relative models are quite advanced [3, 4], while the mechanism of nucleation and coalescence, as well as the associated micromechanics, are less understood even if some papers provide a good description of such mechanisms [5, 6]. It is clear that improving the understanding of the above mechanisms and of their effects on failure modes and fracture resistance will result in a better ease to develop micromechanical prediction tools for the analysis of real components which behave in the nonlinear fracture mechanics field¹.

Among the most promising models introduced in recent years the one proposed by Gurson-Tvergaard (GT) links the propagation of a crack to the nucleation and growth of micro-voids in the material and then is able to connect the micromechanical characteristics of the component under study to crack initiation and propagation up to a macroscopic scale, such model works very well with many metal alloys but not with composites materials whose damages mechanisms are governed by different concepts [7].

The three stages of nucleation, growth and coalescence of micro-voids are well-established results of metallographic observation for polycrystalline metals at ductile failure. The simulation of these microstructural damage processes has been considered in various micromechanical and macro mechanical approaches in the literature.

A macro mechanical model can be obtained by statistical average of microscopic quantities by a homogenization process.

The Gurson model [8], which derived a macroscopic yield function and an associated constitutive flow law for an ideally plastic matrix containing a certain volume fraction of spherical voids, is a well-known analytical approach to this problem.

Empirical modifications of this approach have been proposed to improve the prediction at low fraction of volume void [9] and to provide a better representation of final void coalescence [10].

In this work this model has been selected, and by means of experimental observations and numerical procedures the characteristic parameters have been determined [11, 12].

Once calibrated and validated the numerical propagation model, it has been applied to the FE model of a stiffened aeronautical panel [13], made of aluminium alloy; the aim is

*Address correspondence to this author at the School Department of Industrial and Information Engineering, Second University of Naples, via Roma 29 - 81031 Aversa, Italy; Tel: +39 081 5010 412; E-mail: francesco.caputo@unina2.it

¹The part of the article has been previously published in World Academy of Science, Engineering and Technology 73 2013.

to optimize residual strength of such panel in presence of cracks.

Commonly, optimization methods [14, 15] aim to minimize one or more functions under assigned boundary conditions and by considering possible ranges of variability of the design variables' values; other structural parameters different from design variables are considered as constant. This procedure is not able to consider the variability of the parameters which randomly influence both the manufacturing process and the service conditions and which, in turn, influences the variability of the performance of the product [16]; therefore a special design methodology, based on probabilistic concepts, is necessary, as well as practical design tools such as to make possible to deeply investigate the probabilistic aspects involved in the design process [17]. This approach allows obtaining a robust design, that is a design insensitive to all variations of the main variables, or, what is the same, a design whose statistics are characterized by the smallest standard deviation, as a function of the statistics of input [18].

This approach can be also linked to another very relevant question; the result of an experimental test carried on an assigned structure is the consequence of the particular and real values of all design variables, whose density functions are supposed to be known: when we try to correlate the test results to a numerical simulation procedure, we want in effect to assess, all other aspects stated, which are the values that the design variables had in the real structure tested in that particular experiment.

Based on the "stochastic design improvement" (SDI) technique [19], a homemade procedure, which is able to perform a preliminary robust design of a complex structural component, has been proposed and applied to the improvement of the residual strength of a cracked stiffened panel [20]. Numerical results have been compared with experimental results from literature [21], with the aim to validate them.

DESCRIPTION OF THE HOME MADE SDI PROCEDURE

Both the design aspects focused in the previous section can be effectively dealt by means of an SDI (Stochastic Design Improvement) process, which is carried out by developing several Monte Carlo (MC) series of trials (runs) as well as of the analysis of the intermediate results.

That procedure is in fact an iterative one, both for the generally non-linear behaviour of the structure and because it often happens that the quality level can be expressed more efficiently through the variation coefficients and not by variances, which therefore can vary in the assumed displacement.

A method which is usually very effective is to find in the cloud pertaining to Monte-Carlo first set the trial which gives the nearest result to the target and to centre there a new set of experiments and so on, until a convergence is obtained which is expressed in terms of a distance, admitting that the shape of the cloud of results will not change substantially passing from initial to target values of the results, but will be

only displaced, and that the amplitude of the required displacement can be forecast through a close analysis of the points which are in the same cloud.

It is also clear that the assumption about the invariance of the cloud can be maintained just in order to carry out the multivariate regression which is needed to perform a new step but that subsequently a new and more correct evaluation of the cloud is needed; in order to save time, the same evaluation can be carried out every k steps, but of course, as k increases, the step amplitude has to be correspondently decreased.

It is also immediate that the displacement of the cloud is obtained by changing the mean (nominal) values of the design variables, as in the now available version of the method all statistical distributions are assumed to be uniform, to avoid the crowding of results around the mode value. It is also pointed out that sometimes the process could fail to perform its task because of some physical (engineering) limit, but in any case SDI allows quickly appreciating the feasibility of a specific design, therefore making its improvement easier. From a practical point of view, the user specifies the value that assigned selected output variable has to reach and the procedure determines those values of the project variables which make the mean of the objective variable equal to that of the target. Therefore, the user defines, according to the requirements of the problem, a set of control variables, with an uniform statistical distribution, that is their natural variability, within which they can vary, observing the corresponding physical (engineering) limits. In the case of a single output variable, the procedure evaluates the Euclidean or Mahalanobis distance of the objective variable from the target after each trial.

Then, it is possible to find the trials for which the distance between the values of the objective variables from those of the target ones reached the minimum value: subsequently each project variable is redefined according to a new uniform distribution with a mean value equal to that used in such "best" trial. The limits of natural variability are accordingly moved of the same quantity of the mean to define the same amplitude of the physical variability. Once the design variables have been redefined a new run starts; the iterative process stops when the assigned number of shots is achieved.

The analysis can also stop when the distance from the target reaches a given value, according to a planned criterion. In the most cases, it is desirable to control in real time the state of the analysis, with the purpose to realize if a satisfactory condition has been obtained.

TEST CASE

The procedure described above has been applied on a flat cracked stiffened panel (Fig. 1).

The full panel is constituted by a skin made of Al alloy 2024 T3 LT, divided in three bays by four stiffeners made of Al alloy 7075 T5 L (see Table 1). The longitudinal size (along the applied displacement) of the panel is 1830 mm, the transversal size is 1190 mm and the nominal thickness is

1.27 mm; the stiffeners are 2.04 mm high and 45 mm width. The stiffeners were connected to the skin by 4.0 mm diameter rivets (protruding head type), and a continuous rivet pattern was used [22-24]. Each stiffener was connected to the skin by two rows of rivets in the longitudinal direction. The distance between the stringers is 340 mm (Fig. 1). Many aspects are involved in the mechanical joints as referred by the authors in [25] and [26]; in the proposed model the stiffeners have been considered rigidly connected to the skin, as results of some preliminary analyses by which it has been carried out that in the selected damage configuration the modelling approach of the connection between the skin and the stringers didn't influence the full panel residual strength.

Table 1. Material Properties

Material	E [MPa]	σ_y [MPa]	σ_u [MPa]	Δ_{ult} [%]
2024 T3 LT	71200	366	482	18
7075 T5 L	67100	525	579	16

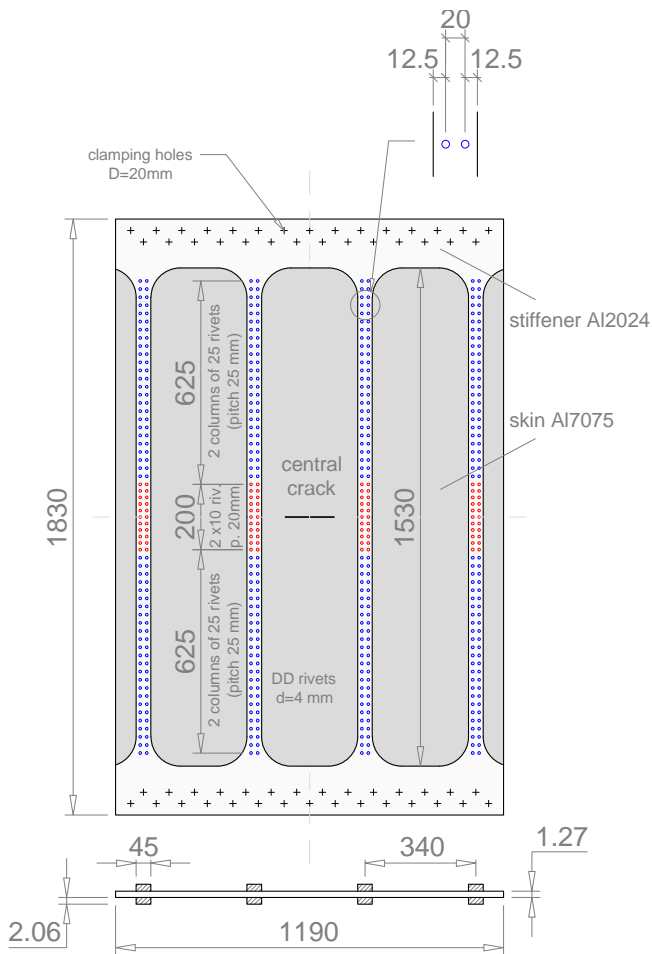


Fig. (1). Flat stiffened panel.

Three different cracked panels have been considered with a central lead through crack equal to 120, 150 and 170 mm respectively. The full panels were tested [21] by considering a test machine with a maximum traction load capacity of 1000 kN. A double-bridge load cell was mounted at the rod

of the actuator. The applied loads were controlled by a typical closed-loop servo system. The stiffened panel was clamped to the testing machine frames by 29 pins per side (20 mm diameter, Fig. 2); the stress field around pins does not reach the bearing strength of the stiffener material. Fig. (2) shows a panel scheme as mounted in the testing frame. Tensile rods were used to prevent horizontal deflection of the frame during loading with care given to the assembly process [27]. The residual strength tests were done under displacement control to make the crack statically grow beyond the point of maximum load. During the residual strength test, the displacement was gradually increased until failure of the panel.

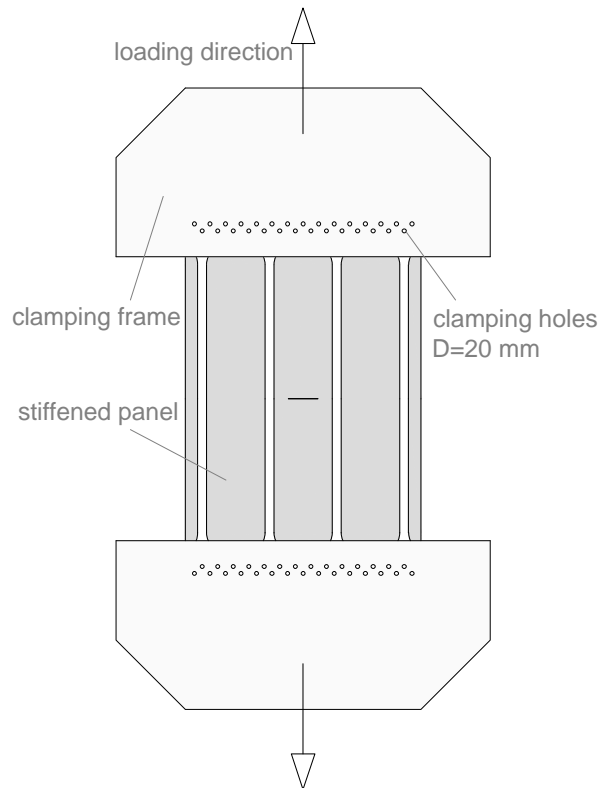


Fig. (2). Testing machine scheme.

A finite element model of the panel has been developed and analysed, by considering the same boundary condition of the experimental test. The numerical model, developed by using the WARP 3D[®] FE code, consists of no. 8400 8-noded 3-dof solid elements and 11450 nodes; only an eighth of the whole structure has been analysed due to the three symmetry planes. Isotropic hardening behaviour has been considered for the material according to the mechanical characteristics reported in Table 1. Crack dimensions and positions were the same of experimental test.

The elements linked to the nodes belonging to the crack plane were modelled by considering a material model based on the Gurson-Tvergaard (GT) model, as implemented in the used code; the GT model is one of the most suitable among the various models based on micro structural aspects

proposed for the description of the crack propagation phenomena in ductile materials.

Each of these elements represents a material unit cell containing an initial cavity fraction; as the stress-strain state increases the volumetric fraction of the cavities decreases, according to the GT model, and when the critical value of cavity fraction is reached, the phenomenon of coalescence starts. From the numerical side, when the coalescence of the cavity starts, the brick elements reduce their ability to model the applied load. Such constitutive model needs a calibration phase as reported in the following paragraph.

NUMERICAL CALIBRATION OF THE GT MODEL PARAMETERS

As generally stated, the Gurson-Tvergaard (GT) model [8, 9] consists of the following expression (1):

$$\phi(q, \sigma_0, f, \sigma_m) = \frac{\sigma^2}{\sigma_0^2} + 2q_1 f \cosh\left(\frac{3q_2 \sigma_m}{2\sigma_0}\right) - 1 - q_3 f^2 = 0 \quad (1)$$

where σ_m is the hydrostatic pressure, σ is the equivalent Von Mises stress, σ_0 is the yielding stress of the material, f is the actual void volume fraction ($f = f_0$ at $t = 0$), q_1 , q_2 and q_3 are the Tvergaard correction factors. The void volume fraction rate, df , consists of two terms, $df_{\text{nucleation}}$ and df_{growth} , which represent respectively linked to the nucleation and the growth of voids. Once reached a certain value of f , say f_c , it is assumed that void coalescence starts, and subsequently a macroscopic crack appears due to the complete “failure” of the material ligaments between voids. From a numerical standpoint, adjacent to the crack growth plane “computational cells” are modelled, in which an algorithm based on the GT expression (1) is implemented; these “computational cells” are numerically characterized by the same parameters of the GT expression (1). By considering one finite element for each computational cell, it follows that the numerical calibration of the GT model parameters and then of the computational cell dimension governs the mesh size [28, 29]. By means of a fitting procedure of numerical results with experimental ones, nine parameters need to be calibrated to fully characterize the computational cell in the sense explained above: the three Tvergaard correction parameters (q_1 , q_2 , q_3); the three parameters associated with the strain normal distribution (mean value, $\bar{\varepsilon}_n$, standard deviation, S_N , and the volume fraction of void nucleating particles, f_N), which are assumed to govern the strain induced voids nucleation rate on the basis of the following expressions (2):

$$df_{\text{nucleation}} = A(\bar{\varepsilon}) d\bar{\varepsilon}_p \quad (2)$$

$$A = \frac{f_N}{S_N \sqrt{2\pi}} \exp\left[-\frac{1}{2} \left(\frac{\bar{\varepsilon}_p - \bar{\varepsilon}_N}{S_N}\right)^2\right]$$

where $\bar{\varepsilon}_p$ is the equivalent plastic strain, D_0 is the initial size of the computational cell and f_0 is the initial volume cavity fraction which can reach its critical value f_c . Another purely numerical parameter, λ , has been considered, which

governs the release model for element forces after the void volume fraction reaches the critical value [30].

Once the critical damage state is reached, at any load step the residual internal forces applied to nodes of the considered element at crack tip, γ , is given by $\gamma = 1.0 - [(D^* - D_0^*)/\lambda D_0]$, where the D_0^* is the average deformed cell height normal to the crack plane when f is equal to f_c , D^* is the actual deformed cell height and λD_0 represents the allowable elongation of the cell size from the critical condition up to the final cell collapse ($\gamma = 0$), with respect to the undeformed cell height² [30]. In any case, beside these parameters, the mechanical properties of the base material (Young modulus, E , Poisson ratio, ν , yielding stress, σ_0 , strain hardening, n), or its stress-strain relationship (σ - ε curve), must be known.

The material considered in the proposed investigation is an aluminium alloy 2024 T3 (Table 1).

The fitting of Tvergaard’s parameters was performed, on the basis of the information available for this material regarding its mechanical properties, by comparing the behaviour of two different numerical models for different opportunely selected boundary conditions; the achieved values are $q_1 = 1.33$; $q_2 = 0.956$ and $q_3 = 1.77$, which confirms the usual assumption $q_3 = q_1^2$. The nucleation phenomena has not been considered in this phase of fitting process and the f_c value has been used only to determine the last point of comparison between the stress-strain curves of the two models without any influence on the fitting process.

The second phase of the calibration process of GT model parameters consists in the determination of the nucleation (ε_N , S_N , f_N) and macro-mechanical (D_0 , f_0 , f_c) parameters. Both a metallographic analysis [11] and an experimental R-curve of the material under examination [21, 31, 32], are necessary in order to successfully develop the second phase of the calibration process. From the metallographic analysis, the defect distribution in the base material can be carried out, which is necessary to choose a first attempt value of the computational cell size, D_0 , and of the initial void volume fraction, f_0 , to be used in the calibration process. As it is possible to observe from the data recorded in Table 2 [11], particles or dispersoids are found, which, as it is known, are one of the causes for void nucleation and therefore can be considered as initial void volume fraction ($f_0 = 2.1\%$). The average distance between the two biggest ($> 10 \mu\text{m}$) particles is $82.89 \mu\text{m}$, which should be approximately the size of the computational cell.

It must be said that the dimensions of the computational cell influence the accuracy of the results, and clearly when smaller is it, better is the numerical-experimental agreement of the results; but if the user wants to analyse full scale structure or big component, a too small size of the computational cell cannot allow a wisdom approach to the analysis due to the increasing of the computational time; therefore, on the basis of the results reported in [33] and of numerical calculations performed by the authors in order to assess those results, a computational cell size $D_0 = 100 \mu\text{m}$

²The part of the article has been previously published in World Academy of Science, Engineering and Technology 73 2013

Table 2. Results From Metallographic Analysis

Eqvdiam [µm]	Vol Fraction	Vol Fraction (st dv)	Nearest Neighbour [µm]	Nearest Neighbour (st dv) [µm]	Min Separation Distance [µm]	Min Separation Distance (st dv) [µm]	Av. Size of Particles in Size Categ
All Sizes	2,10	0,40	8,58	5,37	5,78	5,30	2,38
1:2	0,18	0,06	15,62	10,78	14,05	11,03	1,46
2:3	0,29	0,07	20,95	13,07	18,27	13,33	2,47
3:4	0,33	0,09	28,23	17,69	24,54	18,17	3,44
4:6	0,49	0,14	26,38	14,85	20,82	15,02	4,85
6:8	0,35	0,15	43,01	25,19	35,00	25,76	6,84
8:10	0,22	0,15	69,60	42,43	59,25	43,54	8,85
10+	0,24	0,24	82,89	54,35	67,90	55,79	12,09

has been considered. In order to calibrate f_0 and f_c parameters, numerical data have been fitted to the experimental ones represented by the R-curve of a central cracked plate under remote traction [21], whose dimensions are 500 mm x 500 mm, with a thickness of 1.28 mm and an initial crack size of 99.6 mm (Fig. 3); the obtained final values are respectively 0.025 and 0.12.

In the same phase of parameters calibration, ϵ_N , S_N and f_N values have been determined, obtaining $\epsilon_N = 0.09$, $S_N = 0.045$ and $f_N = 0.11$. The advantage in the use of such a kind of specimen instead of a compact test specimen to characterize experimentally the material toughness is to provide an easier transferring of the evaluated parameters to the considered full scale components [3], avoiding the difficulties due to the yielding scale at crack tip³ [34-36].

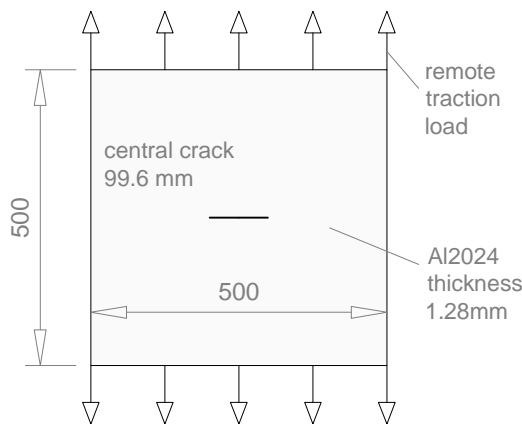


Fig. (3). Fitting parameters panel.

STIFFENED PANEL: EXPERIMENTAL TEST AND NUMERICAL SIMULATIONS

By considering the values carried out by the calibration process of the GT parameters described in the previous section, the R-Curve of the cracked stiffened panel described

in Fig. (1) has been numerically determined, in the same boundary conditions of the experimental tests and in presence of just one crack in the middle bay of initial size a_0 respectively equal to 120, 150 and 170 mm. In Figs. (4-6) the comparisons between numerical and experimental results have been shown; as expected, the numerical results obtained are in good agreement with the experimental ones as proof of the relevance of the model adopted.

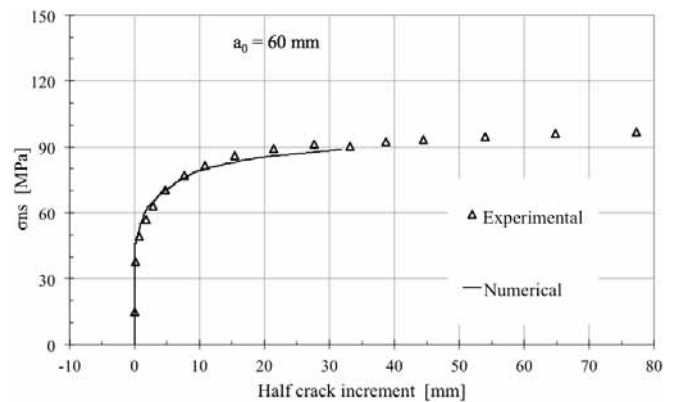


Fig. (4). Stress comparison for an initial crack length of 120 mm.

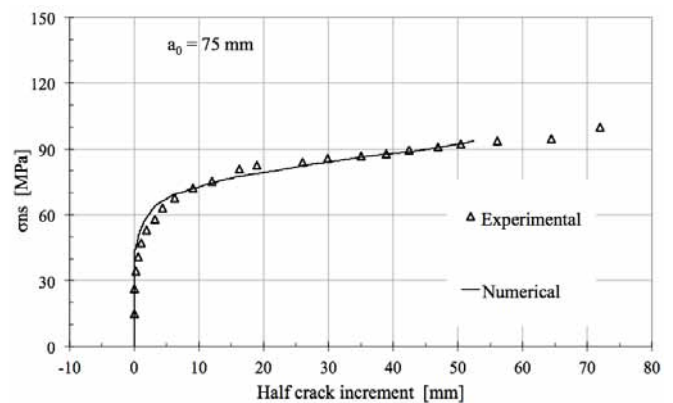


Fig. (5). Stress comparison for an initial crack length of 150 mm.

The same full-scale damaged panel has been used to perform a Stochastic Design Improvement. A through crack 20 mm long set in middle of a bay has been considered.

³The part of the article has been previously published in World Academy of Science, Engineering and Technology 73 2013.

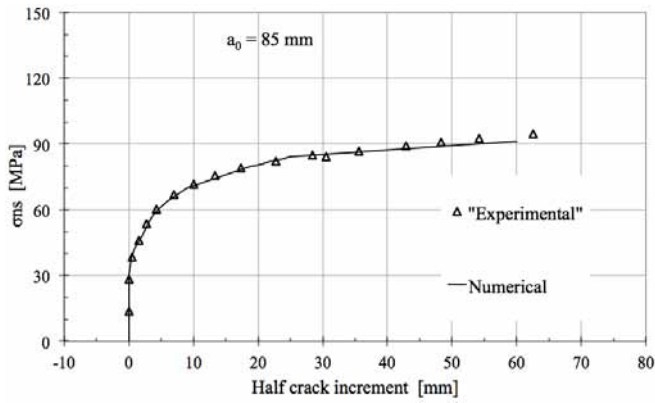


Fig. (6). Stress comparison for an initial crack length of 170 mm.

Only two design variables, stringer’s pitch and height, have been chosen in order to obtain a flexible procedure and most reliable results. Previous work shows [37] an unsatisfactory number of test applications used to assess results of numerical model, so in the current paper more comparison data with other experimental results have been added. Table 3 shows the details of the design variables.

Table 3. Design Variables (% Respect to Initial Value)

Design Variables	Initial Value [mm]	Natural Variability [mm]	Lower Engineering Bound [mm]	Upper Engineering Bound [mm]
Stringer pitch	340	20 (6%)	306 (90%)	374 (110%)
Stringer height	2.06	0.5 (24%)	1.03 (50%)	3.09 (200%)

The procedure can be considered completed when the maximum value of the residual strength curve reaches an increasing of 18% (probability of success greater than 0.85).

RESULTS AND DISCUSSION

In order to successfully complete the application of the proposed SDI procedure on the selected test-case, no. 7 sets of trials (runs) have been executed; each run constituted by no. 36 shots. At the end, more than 250 numerical analyses have been performed. In a second phase of the procedure it has been necessary to execute a supplementary MC test with the aim to assess the results carried out with a poor number of shots per run. A MC statistical analysis has been performed by means of 387 trials reaching a very satisfactory result.

Figs. (7, 8) show the maximum value of the residual stress curve for the two design variables within their engineering variability.

Fig. (9) shows the maximum value of the residual stress curve for each shot; the solid horizontal line represents the initial value of such maximum value (104,5 kN) while the dashed line represents the target of the maximum value of the R-curve (123,3 kN). As it possible to observe during the 6th run, 31 numerical evaluations overcome the target value and reach a percentage of success greater than the requested

one (0.85). In the same figure two vertical dashed lines highlight the trials belonging to the 6th run.

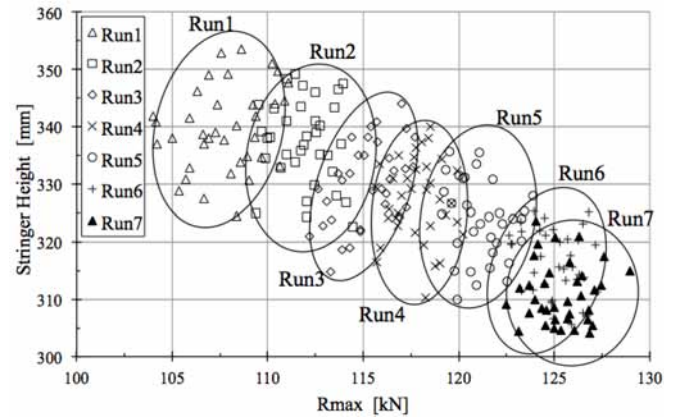


Fig. (7). Design variable vs output variable.

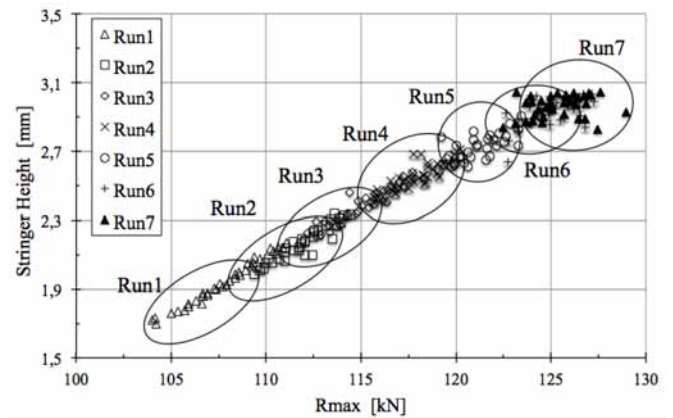


Fig. (8). Design variable vs output variable.

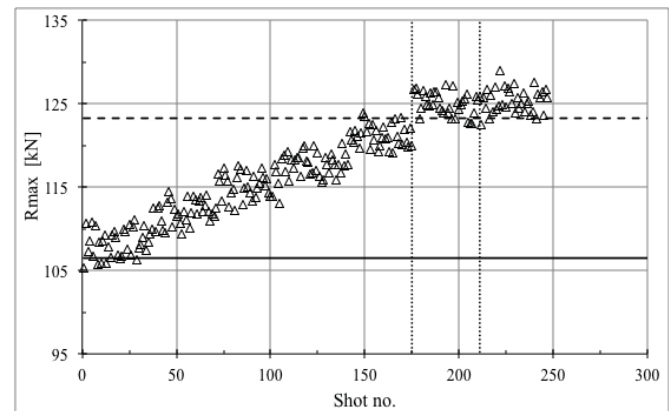


Fig. (9). Output variable vs shots per run.

The design variables within such run assume the following mean values: Stringer Pitch = 316 mm, Stringer Height = 2.94 mm.

At this point it is necessary to perform an extended MC analysis on the base of the results coming from the 6th run. A total of 387 numerical executions have been performed and Fig. (10) shows that 333 trials give a maximum value of the R-curve that overcome the target value. The percentage of success is than 86%.

The comparison between the sixth run and the extended MC analysis (Fig. 11) gives good statistical results in terms

of mean values that are respectively 125,1 kN and 126,8 kN (+1.38%).

Fig. (12) shows the R-curve for the best shot of each run; the reference maximum value of the R-curve is 104,5 kN while the requested target (123,3 kN) has been reached after 6 runs with a probability of success equal to 86%; the seventh run gives a probability of success (92%) greater than the requested one for the present procedure.

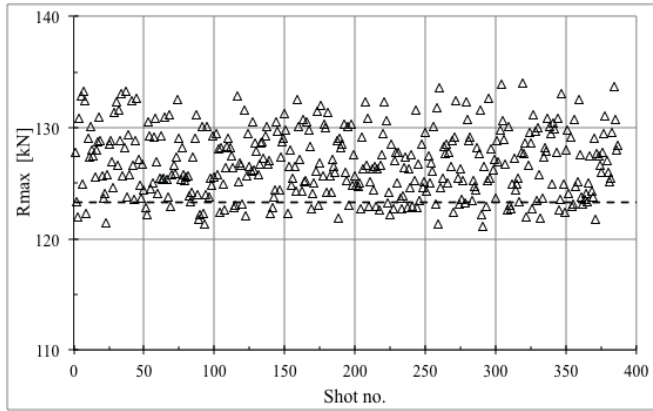


Fig. (10). Output var. vs shots - extended MC.

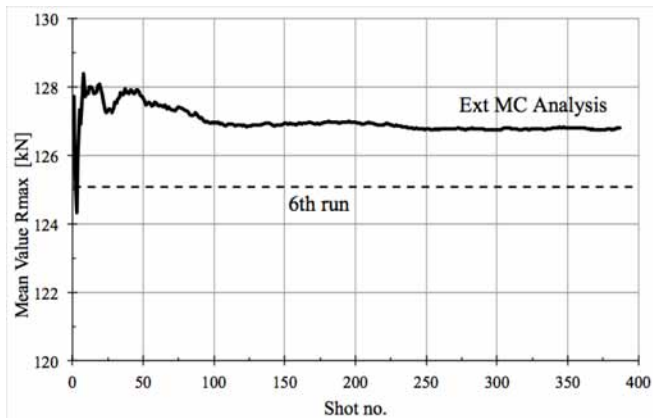


Fig. (11). Mean of output variable vs shots.

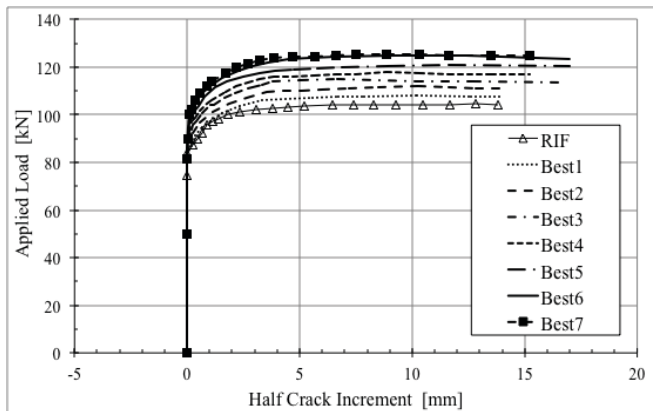


Fig. (12). Mean of output variable vs shots.

CONCLUSIONS

The application of the proposed SDI procedure to improve the residual strength of a full scale flat stiffened cracked panel made of aluminium alloy gave good results even though the selected test case was very complex.

A great starting point, for the success of the whole procedure, is represented by the good numerical-experimental correlation stated in the first part of the work.

The achievement of such result represents a great advantage for this kind of applications also constitutes a guarantee that the final results of the SDI procedure are reliable.

Actually, the used numerical Gurson-Tvergaard micromechanical damage model, in the form implemented in the algorithms of the WARP3D[®] FE code, worked very well to predict the R-curve of the test case, after calibrating its parameters by means of a numerical-experimental correlation of the results.

CONFLICT OF INTEREST

The authors confirm that this article content has no conflict of interest.

ACKNOWLEDGEMENTS

Declared none.

REFERENCES

- [1] Mahnken, "Theoretical, numerical and identification aspects of a new model class for ductile damage", *International Journal of Plasticity*, vol. 18, 2002, pp. 801-31.
- [2] Xia, C. F. Shih, and J. W. Hutchinson, "A computational approach to ductile crack growth under large scale yielding conditions", *Journal of the Mechanics and Physics of Solids*, vol. 43-3, 1995, pp. 389-413.
- [3] O. Chabanet, D. Steglich, J. Besson, V. Heitmann, D. Hellmann, and W. Brocks, "Predicting crack growth resistance of aluminium sheets", *Computational Materials Science*, vol. 26, pp. 1-12, 2003.
- [4] O. Kintzel, S. Khan, and J. Mosler, "A novel isotropic quasi-brittle damage model applied to LCF analyses of Al2024", *International Journal of Fatigue*, vol. 32-12, pp. 1948-59, 2010.
- [5] J. Faleskog, X. Gao, and C. F. Shih, "Cell model for nonlinear fracture analysis – I Micromechanics calibration", *International Journal of Fracture*, vol. 89, pp. 355-73, 1998.
- [6] F. Scheyvaerts, P.R. Onck, C. Tekoğlu, and T. Pardoen, "The growth and coalescence of ellipsoidal voids in plane strain under combined shear and tension", *Journal of the Mechanics and Physics of Solids*, vol. 59-2, pp. 373-97, 2010.
- [7] F. Caputo, G. Di Felice, G. Lamanna, A. Lefons, and A. Riccio, "Numerical Procedures for Damage Mechanisms Analysis in CFRP Composites", *Key Engineering Materials*, vol. 569-570, pp. 111-8, 2013.
- [8] L. Gurson, "Continuum theory of ductile rupture by void nucleation and growth: part I - yield criteria and flow rules for porous ductile media", *Journal of Engineering Materials and Technology - T. ASME*, vol. 99-1, pp. 2-15, 1977.
- [9] V. Tvergaard, "Influence of void nucleation on ductile shear fracture at a free surface", *Journal of the Mechanics and Physics of Solids*, vol. 30, pp. 399-425, 1982.
- [10] V. Tvergaard, and A. Needleman, "Analysis of the cup-cone fracture in a round tensile bar", *Acta Metallurgica*, vol. 32, pp. 157-169, 1984.
- [11] J.S Robinson, Presentation on the IDA meeting in Geesthacht 22-23 June 2005, University of Limerick (2005).
- [12] G. Lamanna, A. Soprano, and F. Caputo, "A numerical investigation on the R-curve of a cracked plate in aluminum alloy 2024-T3", *Journal of Mechanical Science and Technology*, in press, 2013.
- [13] F. Caputo, G. Lamanna, and A. Soprano, "Stochastic improvement of the residual strength of a stiffened panel", *Key Engineering Materials*, vol. 348-349, pp. 301-304, 2007.
- [14] C. Zang, M.I. Friswell, and J. E. Motterhead, "A review of robust optimal design and its application in dynamics", *Computers and Structures*, vol. 83, Ed. Amsterdam, pp. 315-326, 2005.

- [15] E. Murphy, K. L. Tsui, and J. K. Allen, "A review of robust design methods for multiple responses", *Research in Engineering Design*, vol. 16, pp. 118-127, 2005.
- [16] F. Caputo, A. Soprano, and G. Monacelli, "Stochastic design improvement of an impact absorber", *Latin American Journal of Solids and Structures*, vol. 3, pp. 41-53, 2006.
- [17] A. Soprano, and F. Caputo, "Building a risk assessment procedure", *Structural Durability & Health Monitoring*, vol. 2, no. 1, pp. 51-68, 2006.
- [18] R. Citarella, and A. Apicella, "Advanced design concepts and maintenance by integrated risk evaluation for aerostructures", *Structural Durability & Health Monitoring*, vol. 2, no. 3, pp. 183-196, 2006.
- [19] Doltsinis, F. Rau, and M. Werner, "Analysis of random systems", Ed. I. Doltsinis, Barcelona, E: CIMNE 2004, pp. 9-149.
- [20] E. Armentani, R. Citarella, and R. Sepe, "FML Full scale aeronautic Panel under multiaxial fatigue: experimental test and DBEM simulation", *Engineering Fracture Mechanics*, vol. 78, pp. 1717-1728, 2011.
- [21] H. J. ten Hoeve, L. Schra, A. L. P. J. Michielsen, and H. Vlioger, "Residual strength test on stiffened panels with multiple-site damage", report n: DOT/FAA/AR-98/53, U.S. Department of Transportation, USA, 1999.
- [22] G. Lamanna, F. Caputo, and A. Soprano, "Geometrical parameters influencing a hybrid mechanical coupling", *Key Engineering Materials*, vol. 525-526, pp. 161-164, 2012.
- [23] A. Soprano, F. Caputo, and A. Grimaldi, "A numerical Investigation about the effects of the riveting operation on the strength of joints", *Key Engineering Materials*, vol. 348-349, pp. 265-268, 2007.
- [24] G. Lamanna, F. Caputo, and A. Soprano, "Handling of composite-metal interface in a hybrid mechanical coupling", *AIP American Institute of Physics conference proceedings*, vol. 1459, pp 353-356, 2012.
- [25] G. Lamanna, F. Caputo, and A. Soprano, "Effects of tolerances on the structural behaviour of a bolted hybrid joint", *Key Engineering Materials*, vol. 488-489, pp. 565-568, 2012.
- [26] G. Lamanna, F. Caputo, and A. Soprano, "Numerical modelling and simulation of a bolted hybrid joint", *Structural Durability & Health Monitoring*, vol. 7, no. 4, pp. 283-296, 2011.
- [27] G. Lamanna, F. Caputo, F.M. Pannullo, and G. De Angelis, "A methodological approach to the tolerance problems during the assembly process of deformable bodies", *Key Engineering Materials*, vol. 488-489, pp. 557-560, 2012.
- [28] F. Caputo, G. Lamanna, L. Lanzillo, and A. Soprano, "Numerical investigation on LEFM limits under LSY conditions", *Key Engineering Materials*, vol. 577-578, pp. 381-384, 2014. Online available since 2013/Sep/23 at www.scientific.net.
- [29] F. Caputo, G. Lamanna, and A. Soprano, "Crack tip parameters under Large Scale Yielding condition", *Structural Durability & Health Monitoring*, in press, 2013.
- [30] A. S. Gullerud, K. C. Koppelhofer, A. Roy, R. H. Dodds, jr., B. Healy, S. RoyChowdhury, M. Walters, B. Bichon, K. Cochran, A. Carlyle, J. Sobotka, and M. Messner, Warp3D Release 17.3.2 3D Dynamic Nonlinear Fracture analysis of solids using parallel computers, User and theoretical manual, (University of Illinois), 2012.
- [31] F. Caputo, G. Lamanna, and A. Soprano, "Numerical investigation on the crack propagation in a flat stiffened panel", *Key Engineering Materials*, vol. 324-325, pp. 1039-1042, 2006.
- [32] C. Cali, and R. Citarella, "Residual strength assessment for a butt-joint in MSD condition", *Advances in Engineering Software*, vol. 35, pp. 373-382, 2004.
- [33] D. Steglich, T. Siegmund, and W. Brocks, "Micromechanical modeling of damage due to particle cracking in reinforced metals", *Computational Materials Science*, vol. 16, pp. 404-413, 1999.
- [34] F. Caputo, G. Lamanna, and A. Soprano, "The plastic zone size at short cracks tip" *Engineering Fracture Mechanics*, vol. 103, pp. 162-173, 2012.
- [35] F. Caputo, G. Lamanna, and A. Soprano, "An analytical formulation for the plastic deformation at the tip of short cracks", *Procedia Engineering*, vol. 10, pp. 2988-2993, 2011.
- [36] R. Citarella, and M. Perrella, "Multiple surface crack propagation: Numerical simulations and experimental tests" *Fatigue and Fracture of Engineering Materials and Structures*, vol. 28, n. 1-2, pp. 135-148, 2005.
- [37] F. Caputo, G. Lamanna, and A. Soprano, "A strategy for a robust design of cracked stiffened panels", *World Academy of Science, Engineering and Technology*, vol. 73, pp. 765-770, 2013.

Received: September 26, 2013

Revised: October 11, 2013

Accepted: October 11, 2013

© Caputo *et al.*; Licensee Bentham Open.This is an open access article licensed under the terms of the Creative Commons Attribution Non-Commercial License (<http://creativecommons.org/licenses/by-nc/3.0/>) which permits unrestricted, non-commercial use, distribution and reproduction in any medium, provided the work is properly cited.